Applied Geochemistry 159 (2023) 105845

Contents lists available at ScienceDirect

Applied Geochemistry

journal homepage: www.elsevier.com/locate/apgeochem

Porewater profiles of Cl and Br in boreholes penetrating the Mesozoic sequence in northern Switzerland

Paul Wersin [a,*], Thomas Gimmi [a,b], Jin Ma [a], Martin Mazurek [a], Carmen Zwahlen [a], Lukas Aschwanden [a], Eric Gaucher [a], Daniel Traber [c]

[a] Rock-Water Interaction, Institute of Geological Sciences, University of Bern, Baltzerstrasse 1+3, 3012, Bern, Switzerland
[b] Laboratory for Waste Management, Paul Scherrer Institut, 5132, Villigen, Switzerland
[c] National Cooperative for the Disposal of Radioactive Waste (Nagra), Wettingen, Switzerland

ARTICLE INFO

Editorial handling by: Mieke De Craen

Keywords:
Anionic tracer profiles
Argillaceous rocks
Opalinus Clay
Br/Cl ratios
Diffusion
Modelling

ABSTRACT

The analysis of tracer profiles of porewaters is a valuable tool to understand transport processes in argillaceous rocks and to unravel the paleo-hydrogeology of a site. In this contribution, anionic tracers (Cl, Br) from eight boreholes located in three study areas (~20 km apart) penetrating the ~800 m thick Mesozoic sequence in northern Switzerland, were analysed. A specific focus was on the Opalinus Clay, a ~100 m thick homogeneous claystone formation, foreseen as host rock for radioactive waste disposal in Switzerland, as well as its mostly clay-rich confining units. Using porewater extraction methods, such as high-pressure squeezing, advective displacement and aqueous extraction, a unique dataset of spatially highly resolved Cl and Br profiles could be obtained. These show systematic and comparable patterns suggesting common paleo-hydrogeological evolution paths for all three study areas. The scatter in the tracer profiles based on the aqueous extraction data are mostly related to the uncertainty in the estimation of the anion-accessible porosity fraction on one hand and in the water content data in the case of low-porosity calcareous rocks on the other. Differences between the study areas are in line with differences in aquifer characteristics. The current shape of the anion profiles is dominated by diffusive exchange with the bounding aquifers over the last several ten thousands to millions of years, as supported by numerical modelling. The Br/Cl signals also suggest the preservation of older signals related to halite dissolution and highly evolved evaporitic porewaters occurring in evaporite-bearing units of the Triassic. Overall, the adopted methodology has enabled to obtain a unique dataset of anionic tracers at regional scale providing a solid basis for understanding the regional paleo-hydrogeology of siting areas for a potential nuclear waste repository.

1. Introduction

Argillaceous rocks generally have a low permeability and the ability to self-seal upon fracturing (Horseman et al., 1996; Bock et al., 2010), thus acting as barriers (seals, aquitards) to fluid flow and solute transport. For these and other reasons, such rock types (termed clay rocks in the following) are foreseen as host formations for nuclear waste repositories in a number of countries (Altmann et al., 2012). The barrier function of the host rock is an important component in the demonstration of safety of deep geological repositories. In this regard, natural chemical and isotopic tracers in porewater of clay rocks yield important information for the assessment of long-term safety. The analysis of tracer profiles helps to demonstrate that solute transport is governed by slow, diffusive exchange with the bounding aquifers (Patriarche et al. 2004a, 2004b; Gimmi and Waber 2004; Mazurek et al., 2009, 2011, Bensenouci et al., 2014, Hendry et al., 2016, Wersin et al., 2018). Analysis of natural tracers in clay rocks and adjacent aquifers in combination with small-scale diffusion experiments also provide quantitative information on diffusion parameters of the studied rock types and help to unravel the paleo-hydrogeology and paleo-hydrogeochemistry of the site (Mazurek et al., 2009 and references therein).

The analysis of profiles of natural tracers, such as stable water isotopes (^{2}H, ^{18}O) and chloride, has usually been limited to single boreholes, such as for example the Benken and Schlattingen-1 boreholes in northern Switzerland. Based on a few groundwater samples and using simplified hydrogeological boundary conditions, tracer profiles could be adequately modelled considering diffusion only in the aquitard and diffusive exchange with the bounding aquifers (Gimmi and Waber 2004;

* Corresponding author.
E-mail address: paul.wersin@geo.unibe.ch (P. Wersin).

https://doi.org/10.1016/j.apgeochem.2023.105845
Received 17 March 2023; Received in revised form 2 November 2023; Accepted 8 November 2023
Available online 22 November 2023

Gimmi et al., 2007; Wersin et al., 2018). Regarding chloride, whose distribution in the pore space of clay rocks is affected by anion exclusion, the anion-accessible porosity fraction (f_a) needs to be accounted for (Pearson et al., 2003). Often, a constant f_a value of ~0.5 for this anion was considered across the entire sedimentary sequence due to lack of data. This was for example the case in the two aforementioned studies or in the study of a deep borehole in the eastern Paris basin (Bensenouci et al., 2014). It should be noted that the anion-accessible porosity fraction is expected to vary according to the clay content, ionic strength and other variables, as for example shown by Van Loon et al. (2023) and Zwahlen et al. (2023).

An extensive deep drilling programme has recently been carried out in three study areas in northern Switzerland in order to evaluate their suitability for hosting high-level and low level/intermediate level radioactive waste (Mazurek et al., 2023). Nine boreholes yielding >6 km of core material were drilled through a thick Mesozoic sequence comprising argillaceous and calcareous units, in most cases down to the Permian or the crystalline basement. A main focus was the characterisation of the porewater tracers of the Opalinus Clay (OPA), a vertically and laterally homogeneous clay rock foreseen as host rock, and the so-called confining units (generally clay-rich but vertically and laterally more heterogeneous than OPA; Section 2.1). Dense sampling, careful preservation of drillcores and tailored analytical procedures enabled to obtain a unique dataset in terms of mineralogy, petrophysical parameters and porewater composition. In particular, porewater natural tracer profiles with an unprecedented spatial resolution could be acquired, including stable water isotopes, Cl, Br and He as well as $\delta^{37}Cl$ in some of the boreholes. In addition, groundwaters from the aquifers over- and underlying the clay-rich sequence were sampled and analysed where possible. Compared to previous studies focussing on single boreholes, this massive dataset has enabled to get a much more comprehensive view on the spatial distribution of the analysed tracers on a regional scale, both vertically and laterally. The addition of the horizontal dimension to the dataset offers new perspectives in the understanding of solute diffusion in three dimensions and not only in individual vertical profiles.

In this contribution, we discuss Cl and Br profiles, as well as Br/Cl ratios. The analysis of Br and Br/Cl profiles is a novel aspect with regard to previous studies in the area (Benken and Schlattingen-1 boreholes, (Nagra, 2001; Wersin et al., 2016)) and helps to improve the knowledge on the paleo-hydrogeological and paleo-hydrochemical evolution of the study areas. The majority of the anion data was obtained from aqueous extraction. For scaling these data to *in-situ* porewater, the anion-accessible porosity fraction needs to be estimated which was done on the basis of a new approach detailed in Zwahlen et al. (2023). The aqueous extraction data were complemented with two direct porewater extraction methods, namely high-pressure squeezing and advective displacement, as detailed in Kiczka et al. (2023). The relevance of diffusive transport is shown by one dimensional vertical transport simulations for simplified scenarios. A more extended modelling study including all profiles and available tracers is in preparation. The overall objective is to understand solute transport processes in the studied Mesozoic sequence in general and more specifically in the OPA and its confining units clay-rich units adjacent to the OPA) on a regional scale. A second objective is to improve knowledge on paleo-hydrogeology and paleo-hydrochemistry in the three study areas. The profiles of stable water isotopes (δ^2H, $\delta^{18}O$) and He are discussed in companion papers (Gimmi et al., 2023; Rufer et al., 2023). Data on the porewater composition (other than Cl and Br) are discussed in Kiczka et al. (2023).

2. Geological, structural and hydrogeological setting

2.1. Lithostratigraphy and tectonic situation

Two of the investigated study areas, namely Jura Ost (JO) and Nördlich Lägern (NL), are located in the Deformed Tabular Jura (north of the front of the Jura Fold-and-Thrust Belt but still affected by thrusting). The third study area, Zürich Nordost (ZNO), largely lies in the Tabular Jura covered by Tertiary Molasse deposits and is barely affected by thrusting (Fig. 1). Two boreholes (BOZ1-1 and BOZ2-1) were drilled in JO and four boreholes (BAC1-1, BUL1-1, STA2-1, STA3-1) in NL. ZNO was investigated by three boreholes (TRU1-1, MAR1-1, RHE1-1), which complement the older boreholes at the Benken (BEN) and Schlattingen (SLA-1) sites, the latter being outside of the study area (Fig. 1). Note that for the inclined RHE1-1 borehole no anion data were collected.

Lithostratigraphic profiles for each of the study areas are illustrated in Fig. 2. The basement (either crystalline or Permian sedimentary rocks) is overlain by the gently SE-dipping Mesozoic sequence with its alternations of shallow marine, coastal or continental deposits of the Triassic at its base. These mainly include dolostones, limestones and evaporitic beds of anhydrite and halite (locally dissolved). The Klettgau Formation (Keuper) at the top of the Triassic is lithologically heterogeneous on the metre scale (dolostone-sandstone-marl-claystone). The overlying open-marine Liassic and Dogger units are generally clay-rich but nevertheless lithologically diverse by means of variable contents of clay minerals, quartz and carbonates (mainly calcite). In particular, the thin Liassic sequence is highly heterogeneous in the vertical dimension (claystone-marl-limestone-sandstone) but much less so laterally. The Opalinus Clay constitutes the most clay-rich unit and shows little lithological variability in both vertical and lateral dimensions. In contrast, the Dogger units overlying the Opalinus Clay show substantial vertical and lateral heterogeneity. In the ZNO and the NL areas, clay-rich units dominate, however, the latter area additionally comprises a rather thick coral reef ('Herrenwis Unit') that is present in the eastern part (Fig. 2). Towards the west, a change towards calcareous lithologies is observed in the JO area where partly oolitic limestones (Hauptrogenstein) dominate in the upper part of the Dogger. The overlying Malm is composed of marls and massive limestones throughout the entire investigated region.

The study areas, which were selected to potentially host a deep geological repository, do not contain any major faults but are bounded by such structures in several cases (Fig. 1). The WSW-ENE-running thrust faults are related to compressional tectonics linked to the Jura Fold-and-Thrust Belt, whereas NW-SE-striking normal faults NE of the ZNO area are associated with the Cenozoic rift system of the Hegau-Bodensee Graben.

2.2. Hydrogeology

Regional and/or local aquifers constitute boundaries of the clay-rich low-permeability Lias-Dogger sequence (Traber 2013; Gmünder et al., 2013; Nagra 2014; Waber et al., 2014; Waber and Traber 2022). They include aquifers in the Malm, consisting of fractured and karstified massive limestones, or (in more western regions) in the Hauptrogenstein located in the upper Dogger. The Triassic Keuper aquifer is not ubiquitously present across the investigated regions. In contrast, the underlying Triassic Muschelkalk (MK) aquifer, consisting of porous and fractured dolostones, is of regional extent. The flow systems are strongly affected by the outcrop zones in the north of the study area (southern flank of the Black Forest Highlands, Tabular Jura) acting as recharge and the major river valleys (Aare, Rhine) acting as discharge areas.

For the Malm aquifer, the northern zone is characterised by young, comparably low mineralised waters. Not only lateral recharge but also vertical recharge from the overlying Molasse deposits locally plays a role (Waber and Traber 2022). For the areas ZNO and NL, the area south of the Rhine river is of major interest. The groundwaters are of the general Na–Cl type which are interpreted as mixtures of a preserved Tertiary marine-brackish water with a younger meteoric water. The Na–Cl component has a residence time in the range of 10^6 a (Waber et al., 2023). Typical hydraulic conductivities of the sections sampled for groundwater are around 10^{-8} m/s.

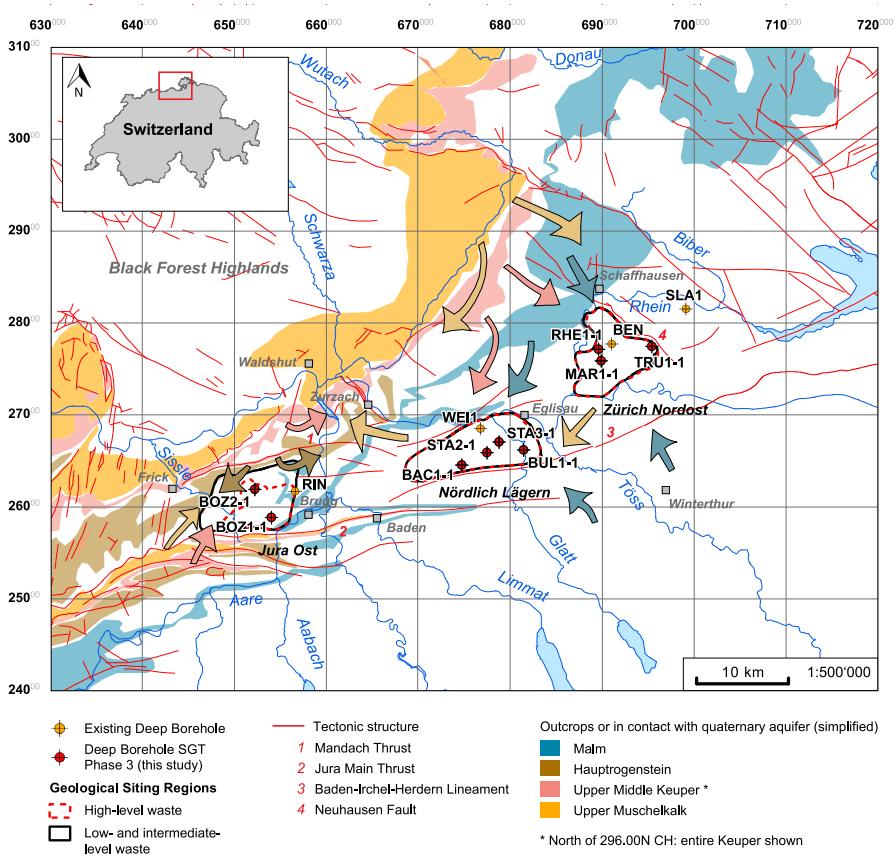

Fig. 1. Map of locations of study areas, boreholes, tectonic structures, and outcrop areas. Simplified flow directions (mainly related to infiltration; no relation to flow velocity) in the Malm, Hauptrogenstein, Keuper and Muschelkalk aquifers are also shown by arrows (based on Gmünder et al., 2013).

In the western area JO, the Hauptrogenstein aquifer is the nearest potential aquifer above the host rock. However, owing to the facies transition from the carbonate platform in the west to clay-rich units in the east, the hydraulic properties vary. In addition, the flow systems are strongly affected by the local topography and the structural setting.

In the upper Keuper, local-scale aquifer systems can exist (Fig. 2) depending on the local lithofacies of the rocks and their hydraulic conductivities. In the ZNO area, the boreholes evidenced a dolomite breccia with hydraulic conductivities up to 10^{-6} m/s (Schwarz et al. 2021a, 2021b). The recharge area is located in the north. This lithofacies was not observed in the area NL. Here, some boreholes showed hydraulic conductivities that allowed for groundwater sampling related to sections with fluvial sand channels (Schwarz et al. 2021c, 2022a, 2022b). In JO, the Keuper aquifer is probably related to a several meters thick dolostone layer. Only in one of two boreholes the hydraulic conductivity was sufficiently high for groundwater sampling (Schwarz et al. 2022c, 2022d).

In the eastern areas ZNO and NL, the Muschelkalk aquifer is a thick fractured and partly porous aquifer with typical hydraulic conductivities in the order of 10^{-7} m/s. From the recharge area in the north to northeast, groundwater evolution can be followed over tens of kilometres to the regional discharge area in the lower Aare valley. Typical groundwaters in the area of interest recharged during cold climate conditions in the Late Pleistocene. For JO, the Muschelkalk aquifer is present as well, but affected by local topography and tectonic structures. In all study areas, an additional deeper aquifer system exists in the Buntsandstein, in combination with the crystalline basement.

3. Methodology

3.1. Core sampling

The strategy, organisation and workflow of drillcore sampling and on-site conditioning is extensively described in Rufer and Stockhecke (2021). Here we describe briefly the sampling procedures relevant to the presented porewater data.

Samples were taken at high spatial/vertical resolution across the entire cored section, with typical sample spacing of 3–6 m in the Lias-Dogger section and 6–12 m in the Malm and Triassic units. Drillcore samples were ~25 cm long with a diameter of 9.5 cm. Furthermore, core samples were taken at specific locations for high-pressure squeezing, advective displacement and other purposes. A precise sampling protocol was adopted to ensure preservation of *in-situ* conditions of the porewater and to minimise (i) drilling-induced contamination, (ii) desaturation and (iii) oxidation of the drillcores. Times of the core conditioning steps were kept as short as possible, leading in most cases to ~20–30 min from retrieval to packaging the cores in vacuum-sealed plastic-coated aluminium bags. All samples were kept cooled to 4 °C at all times during on-site storage, transport to the core storage centre and further to the RWI group at the University of Bern. Some samples from the TRU1-1 and BOZ2-1 boreholes were transported to BRGM (Orléans, France) where they were analysed for a number of parameters, including also aqueous extraction for Cl and Br as well as petrophysical data. The procedures of drillcore handling for petrophysical, mineralogical, porewater and gas analyses in the respective labs are detailed in RWI (2020).

3.2. Petrophysical and mineralogical data

Prior to preparation, samples were removed from the cooling room

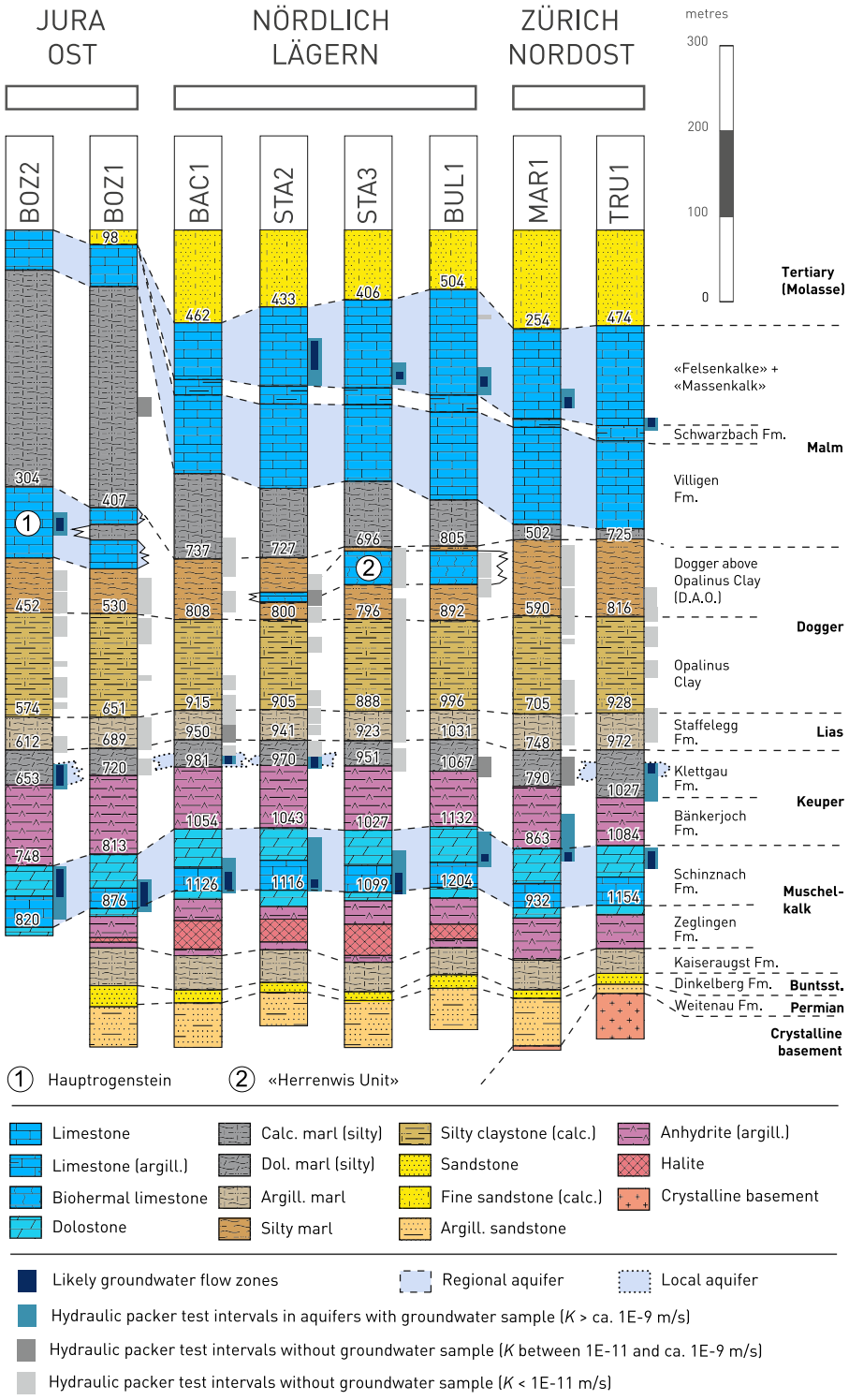

Fig. 2. Simplified lithostratigraphic profiles of vertical boreholes in the three study areas, arranged from W (left) to E (right). Numbers indicate depths of selected stratigraphic boundaries in m below surface. Note that no hydraulic testing was performed in the Buntsandstein/crystalline basement and in the Tertiary Molasse sections, both of which may include horizons with enhanced permeability.

and stored overnight at ambient temperature. After opening the protective wrapping, samples were prepared and conditioned within 15–20 min, in order to minimise the effects of oxidation and evaporation. First, core rims of ~2 cm were rapidly removed by chisel and hammer, and only the saturated, uncontaminated material from the central parts of the core was used for petrophysical and porewater studies. Water content was obtained from drying of about 200 g rock chips at 105 °C until weight constancy. Porosity was calculated from the water content and, alternatively, from measured bulk wet and grain densities. Bulk mineralogical composition was quantified by a combination of X-ray diffraction and chemical data (S, C_{inorg}, C_{org}). Clay mineralogy was obtained from X-ray patterns of the <2 μm fraction. Details pertinent to methods and procedures are provided in RWI (2020).

3.3. Cl and Br data

Aqueous extraction tests (AqEx) were conducted according to the following workflow: Rock material from the central parts of each core was disintegrated to small pieces of a few mm^3 each. 30 g of rock were added to 30 g of degassed (N_2 purged) ultra-pure water and reacted for 24 h in an anaerobic glovebox (95:5 N_2:H_2 atmosphere equipped with two Pd catalysts). After extraction, suspensions were centrifuged and then filtered by 0.2 μm PES filter outside the glovebox. The filtrates were then analysed for anions (Cl, Br, SO_4, NO_3, F) and – for most boreholes – cations (Na, Ca, Mg, K, Sr, NH_4) by ion chromatography (Metrohm 850 Professional IC), but only Cl and Br are reported here. For anion analyses, a Metrosep ASupp7-250/4.0 column (Nr. 6.1006.630) and a 3.6 mM Na_2CO_3 eluent solution was used. Analytical uncertainties were ±5 % and ±4 % for Cl and Br, respectively. Aqueous extraction tests using saturated rock samples (the standard workflow) yielded similar results for Cl as those conducted with material dried under atmospheric conditions, except for organic-rich samples from the Staffelegg Fm., where drying at 105 °C led to considerably lower Cl and, even more so, Br concentrations. It is suspected that oxidation and/or drying at high temperatures triggers some sort of interaction between anions in solution and organics. For these samples, the aqueous extract on saturated material was used to constrain the porewater concentration. The concentrations of Cl and Br were re-calculated to contents in bulk porewater by considering the solid-to-liquid ratio based on the water content measured on adjacent aliquots.

High-pressure squeezing (SQ) of selected cores was performed at pressures of 200–500 MPa to extract and analyse porewaters. The procedures of these squeezing tests, which were conducted at the Central Research Institute of Electric Power Industry (CRIEPI, Japan), are detailed in Kiczka et al. (2023). Here only the tests at the lowest squeezing pressure, thought to represent *in-situ* conditions most closely (Mazurek et al., 2015; Kiczka et al., 2023) are reported. Porewaters obtained at each pressure step were collected and stored at 4 °C and then sent to the RWI group at the University of Bern for chemical analysis. Squeezed rock samples were subsequently subjected to aqueous extraction according to the procedure described above in order to obtain the inventories of Cl and Br and to estimate the anion-accessible porosity fractions. Squeezed waters and aqueous extracts were analysed for major ions with the IC method. Analytical uncertainties were ±5 % and ±4 % for Cl and Br, respectively.

Advective displacement (AD) was another method that was used to extract and analyse porewaters. The procedures of this method are detailed in Mäder (2018) and Kiczka et al. (2023). A large hydraulic gradient was applied to a confined rock sample of ~8 cm length, by which porewater was displaced by artificial porewater (spiked with tracers) injected from the bottom. The displaced porewater samples with volumes of a few hundreds of μL up to 3 mL were collected. After discarding the first syringe the next two syringes were considered to best reflect *in-situ* porewaters and these data are reported here. Aqueous extraction on saturated core material adjacent to the AD core was also carried out according to the procedure outlined above. These extracts and the advectively displaced waters were subsequently analysed for major ions with the IC method. Analytical uncertainties for Cl and Br were the same as for squeezed waters.

Estimation of anion-accessible porosity: Chloride and bromide are considered to behave as conservative species in the porewater with no or limited interaction with the minerals. In argillaceous rocks, anions are repelled from the negative structural charge of the clay-mineral surfaces and are thus affected by ion exclusion. In other words, they only occupy part of the total water-filled porosity, the fraction of which is often termed anion-accessible porosity (Pearson 1999; Pearson et al., 2003). Anion concentrations decrease gradually with decreasing distance to charged surfaces, but the simplified concept of used here considers just a binary distinction of anion-accessible and anion-inaccessible porosity (cf. Zwahlen et al., 2023).

Advective displacement (AD), squeezing (SQ) and diffusion (DI) experiments produce specific anion-accessible porosity fraction (f_a) data (as detailed in Zwahlen et al., 2023). In AD and SQ experiments the f_a values were calculated by dividing the Cl concentration in bulk porewater (obtained from aqueous extracts) of the respective samples by the 'free' porewater concentration from the AD and SQ experiments (Kiczka et al., 2023). In DI experiments, the f_a values were calculated from species-specific porosities obtained from through-diffusion experiments using tritiated water (HTO) and ^{36}Cl (Van Loon et al., 2023). Representative relative errors of f_a are 20% for the Malm, 15% for the Dogger above Opalinus Clay and 10% for the Opalinus Clay. The final uncertainty was derived from error propagation of the individual errors on the concentration in aqueous extract, the water content and the f_a value. The measured f_a values fed into two empirical models used to scale the bulk porewater profiles to 'free' porewater profiles: (1) Formation- and member-specific averaging model (2) clay-content model (see Zwahlen et al., 2023). The formation- and member-specific averaging model uses averages of AD, SQ and DI data and was developed for the Jurassic sections of the profile. For BOZ1-1 and BOZ2-1, which display the most dilute porewaters in the Jurassic section, the f_a values obtained from diffusion data on one hand and from AD and SQ on the other hand deviated considerably, in particular in the OPA. This was accounted for by considering two variants in this formation: the first variant considered f_a data based on diffusion data, whereas the second variant considered f_a values derived from AD and SQ data. Note that in other boreholes with higher ionic strength in the porewaters, no such deviation was found between the diffusion and AD/SQ datasets. This issue is discussed in more detail in Zwahlen et al. (2023). The clay-content model assumes a dependency of f_a on the clay-mineral content. It is defined by a constant average f_a from AD, SQ and DI data above a defined clay-mineral content (30 %) and includes an extrapolation of f_a from this constant value to f_a of 1 at zero clay-mineral content. This clay-content model was applied to the Triassic sections where the averaging model (1) could not be used due to lack of data. Note that the f_a values were derived from Cl data and used for the construction of both Cl and Br profiles.

Data on aqueous extraction, water contents, the anion-accessible porosity fractions, squeezing, advective displacement and groundwater are listed in Appendix A1-A3 (SM).

3.4. Groundwater sampling & analysis

Groundwater samples were taken from packed-off intervals of the aquifers of the Malm, Hauptrogenstein, Keuper and Muschelkalk during hydraulic testing. In some packed-off intervals, no reliable sample could be retrieved, which is related to low hydraulic conductivity. Note that drilling mud and test waters were traced with different dye tracers, such as uranine and Na-Naphthionate or 1.5-NDSA (Lorenz et al., 2022) in order to identify the degree of contamination of the *in-situ* groundwater. Pumped groundwaters were monitored for temperature, pH, electrical conductivity, O_2, redox potential and dye concentrations. As soon as on-site measurements indicated stable physico-chemical parameters and low degrees of contamination, a final groundwater sample was withdrawn, often with a contamination of <1%. In some cases, considerable contamination remained, and this required a numerical correction procedure. A large suite of chemical and isotopic parameters were measured in the laboratory. Cl and Br were measured with IC. The analytical uncertainty varied within 3–6 %.

3.5. Modelling

Transport of Cl and Br across the formations between the Malm and Muschelkalk was modelled using the numerical code PFLOTRAN (www.pflotran.org). When modelling an earlier obtained tracer profile across Opalinus Clay in the ZNO area Gimmi and Waber (2004) and Gimmi et al. (2007) identified diffusion as the dominant transport process.

Thus, only diffusion was considered in the current model. However, different to the mentioned earlier Benken study, porosities and pore diffusion coefficients were varied with depth according to Cl diffusion results (Van Loon et al., 2023), porosity measurements (Mazurek et al., 2023), and temperature logs (details shown in Appendix B1, SM).

At this stage, only highly simplified hydrologic scenarios for the more recent past were considered for modelling. We focus here on BOZ2-1, STA2-1 and TRU1-1, which are all clearly influenced by the Keuper aquifer below the Opalinus Clay and an aquifer in the upper part. The simulations presented here for the three profiles serve as typical examples for the simplified scenarios. The porewater composition in the Opalinus Clay formation was taken as basis for the initial condition of our simulations, which should approximate an old formation water having a uniform composition across the modelled depth interval. The top and bottom boundary conditions were set to arbitrary values fitting the general trend of the initial tracer profiles in order to mimic an "old" composition within the Malm/Hauptrogenstein and the Muschelkalk aquifers. After having obtained a reasonable match between the modelled and measured tracer profiles inside the Opalinus Clay, the various aquifer boundaries were activated by fixing their composition to the present-day values in several steps. Step function changes were used because it was demonstrated for the Benken borehole that slowly changing boundary conditions did not lead to a good match with the data (Gimmi et al., 2007). Further details are given in Appendix B1 (SM).

Here, the evolution of the profiles was simulated based on times of changes of boundary conditions derived from water isotope tracers (Gimmi et al., 2023). Although we have little knowledge about events from the more distant past, the resulting times provide valuable information of more recent events, particularly in the Keuper aquifer. A broader modelling study is currently ongoing, which will evaluate a number of different scenarios in more detail.

4. Results and discussion

4.1. Chloride profiles

Chloride concentrations obtained from squeezing (SQ), advective displacement (AD) and aqueous extracts (AqEx) as well as from sampled groundwaters are shown as a function of depth across the drilled Mesozoic sequence in Fig. 3. Overall, well-constrained profiles with consistent SQ, AD and AqEx porewater data are identified. Moreover, the groundwater data are similar to the porewater data in the corresponding depth intervals. Note that the errors on AqEx data are larger than for the direct extraction methods because they require recalculation to Cl-accessible porosity. The propagated error on the recalculated concentration comprises the errors on the concentration in the extract solution, the water content and the anion-accessible porosity fraction. It should be pointed out that for the latter a general conceptual uncertainty pertains (see section 3.1). Moreover, relative uncertainties in water contents increase in low porosity rocks. This is evident in the Triassic rocks in the lower part of the sequence and results in considerable variations of the calculated *in-situ* concentrations (Fig. 3). To a large degree, this can be explained by the fact that aqueous extraction and water-content determination were obtained from immediately adjacent but not identical materials, so small-scale heterogeneity may be an issue. In the upper part of the sequence, generally less scatter is noted and profiles tend to be smoother. Some variation is manifested in the upper and lower clay-rich confining units which are both vertically and laterally more heterogeneous than the Opalinus Clay. In this context, the 'Herrenwis Unit' in the middle Dogger (reef facies), a low porosity limestone-rich rock with strong variations in clay content, is worth mentioning. As discussed by Zwahlen et al. (2023), the estimation of meaningful anion-accessible porosities poses a challenge for this heterogeneous unit, which occurs in parts of the NL study area, and accordingly the scatter in Cl concentrations is considerable in this unit.

Study area JO: The shape of the Cl profiles based on aqueous extraction depends on the choice of the anion-accessible porosity fraction, given the fact that the values obtained from SQ and AD experiments differ markedly from those obtained from diffusion experiments, unlike in the other study areas where results from all methods converge (lowest ionic strength in JO; see discussion in Zwahlen et al., 2023). Considering the data based on diffusion, maxima are found in the Opalinus Clay (3–4 g/L), with marked decreases up- and downwards. Considering the SQ/AD data, flat profiles result at concentrations of 2–3 g/L. In BOZ2-1, Cl concentrations decrease upwards to reach a distinct minimum in the Hauptrogenstein aquifer. In BOZ1-1, this unit shows low permeability, and Cl remains around 3 g/L up to the Malm limestones. In the underlying Liassic, Cl concentrations decrease strongly towards the Keuper aquifer. In the case of BOZ1-1 no groundwater sample could be extracted, but the tracer profile clearly indicates the presence of this aquifer.

In the lower part of the sequence of BOZ1-1, Cl concentrations show an increasing trend with depth (but with considerable scatter) towards the Muschelkalk aquifer where the groundwater exhibits a Cl concentration of ~9 g/L. The increase continues even below the aquifer, reaching more than 100 g/L at a depth of 880–910 m. These concentrations are probably influenced by a halite layer located at 914 m depth (Wersin et al., 2022).

Study area NL: In the Opalinus Clay, the Cl profiles in all four boreholes are flat and show little scatter, indicating a long-term diffusive equilibration and the absence of geologically young disturbances. Mean concentrations range between about 7 (STA2-1) and 13 (BUL1-1) g/L. Note that these two boreholes are only 2.8 km apart, so there is a marked lateral gradient of Cl concentration. In the Dogger above the Opalinus Clay, the Cl data show a substantial scatter in boreholes STA3-1 and BUL1-1, which is mainly due to the presence of the heterogeneous reef limestones of the 'Herrenwis Unit'. This scatter is likely not real but due to uncertainties related to estimating the anion-accessible porosity fraction in this unit. The Br/Cl profiles at this level show much less scatter because they do not depend on any assumptions regarding anion accessibility (see below). In the Malm, Cl concentrations remain constant or decrease slightly, and they show good consistency with the sampled groundwaters.

The presence of the Keuper aquifer (with $K \geq 1 \times 10^{-8}$ m/s), occurring only in the western boreholes (BAC1-1, STA2-1), and the substantial heterogeneity of Cl concentrations in the underlying Muschelkalk aquifer (<1 g/L in STA2-1 to 86 g/L in BUL1-1) explain the variation of the Cl profiles in the porewaters in the Triassic sections. The groundwater concentrations fit well with those of adjacent porewaters within error. The brine in the Muschelkalk aquifer of BUL1-1 is the most saline water known for this aquifer in northern Switzerland and is explained by dissolution of halite that is present below the aquifer.

Study area ZNO: Cl concentrations in the Opalinus Clay show little scatter but a weak decrease with depth. A decrease is also identified towards the Malm aquifer (data available only for TRU1-1). A sharper decrease to values < 1 g/L is observed downward towards the Keuper aquifer, with substantial scatter (at least partially due to the mentioned methodological issues) at deeper levels. The high Cl levels observed in the Lower Muschelkalk of MAR1-1 can be reasoned as a result of the dissolution of halite. In fact, a salt solution horizon at a depth of 981–985 m depth has been identified in the MAR1-1 borehole (Pietsch, pers. communication). Let us note that the profile shapes as well as the absolute concentrations are quite similar to those in the older boreholes Benken and Schlattingen-1 (see Fig. 1 for localisation; data in Gimmi and Waber 2004; Wersin et al., 2016). These could be explained by diffusive exchange with the Keuper and Malm aquifers during the last 0.5–1 Ma based on numerical modelling (Gimmi et al., 2007; Wersin et al., 2016, 2018). The regional homogeneity between Malm and Keuper aquifers is also corroborated by the isotope profiles of $\delta^{18}O$ and $\delta^{2}H$ (Gimmi et al., 2023). It is remarkable to find such homogeneous conditions over large distances (11 km between MAR1-1 and Schlattingen-1). Moreover, the Schlattingen-1 borehole is separated from the others by the regional,

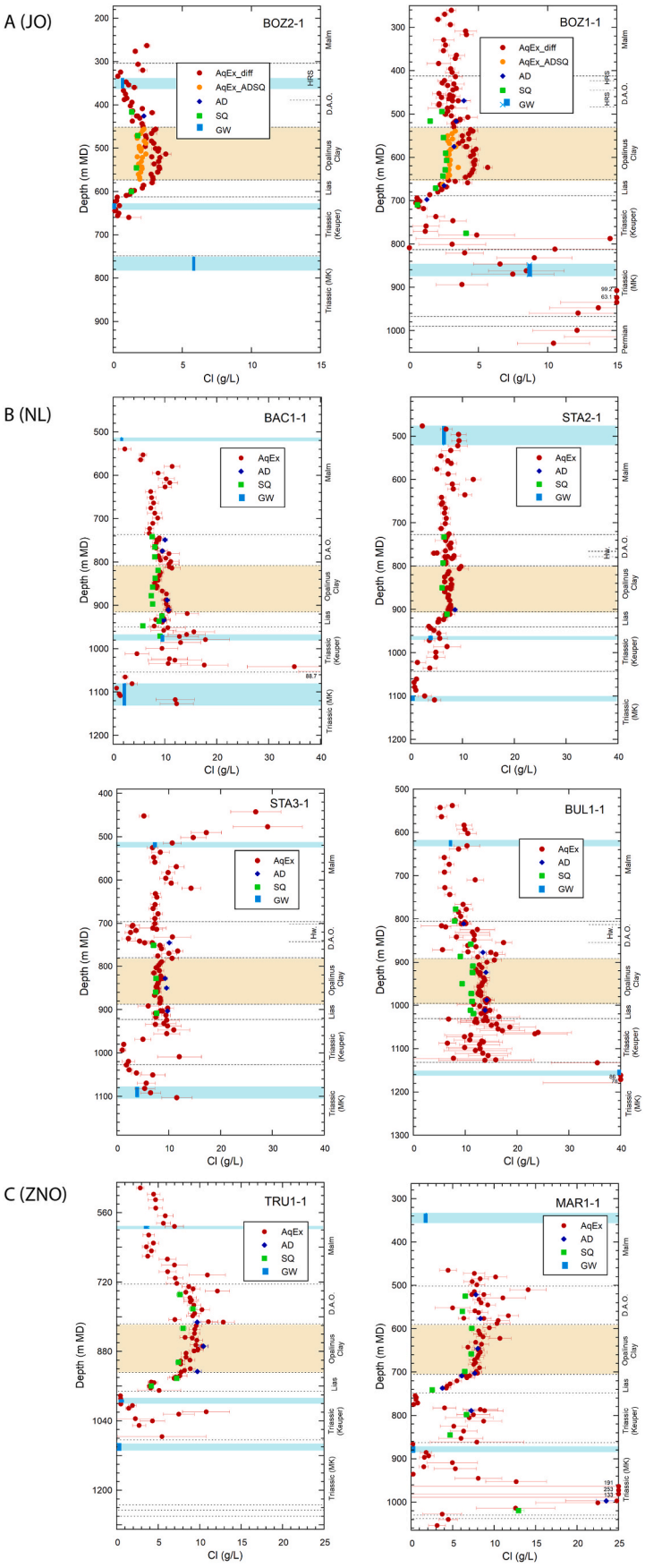

(caption on next page)

Fig. 3. Cl profiles for study areas JO (A), NL (B) and ZNO (C). Opalinus Clay highlighted in beige. Note site-specific scaling of x-axis. Note that highest concentrations in the Lower Muschelkalk (~100–150 g/L) in MAR1-1 are outside of the plot. For JO boreholes, two variants for scaling of the AqEx (aqueous extraction) data are shown as detailed in the text. Blue bars for groundwater represent best estimates for the position of major inflow zones. AD: advective displacement data, SQ: squeezing data, GW: groundwater data. MK: Muschelkalk, D.A.O.: Dogger above Opalinus Clay, HRS: Hauptrogenstein, Hw.: 'Herrenwis Unit'. Groundwater data are preliminary, minor changes for final data due to additional correction procedure for drlling fluid contamination are possible.

NW-SW striking Neuhausen Fault (Fig. 1), but apparently this has no effect on the distribution of salinity in the aquifers and in the aquitard sequence.

In summary, Cl concentrations in the Opalinus Clay, i.e. in the centre of the aquitard, are constant in each borehole or show only a minor trend with depth. The scatter of the data is remarkably low. Concentrations are lowest in the study area JO (2–4.5 g/L). In area NL, they are in the range of 7–13 g/L, and in the area ZNO 8–9 g/L are identified. While no systematic lateral trends of Cl concentration are found (except the low values in JO), there is a conspicuous correlation with current depth of the formation (Fig. 4). This could be related to a loss of salinity from the originally marine porewater composition towards the surface, or also to an input of salinity from below. The shapes of the Cl profiles across the Mesozoic are conspicuously similar in study area ZNO (also considering data from the older boreholes Benken and Schlattingen-1) but differ markedly in the study area NL.

4.2. Bromide profiles

Bromide profiles are shown in Fig. 5 for all boreholes. In qualitative terms, they are similar to those of Cl, but the scatter is somewhat larger, likely due to the low concentrations that in part are close to the limit of quantification in the case of aqueous extracts. In particular, this is often the case in the low-porosity rocks in the Triassic, where the propagated errors are large. Br concentrations in the Opalinus Clay and adjacent units are distinctly different between boreholes of the NL study area, whereas they are comparable in the other two areas. As for Cl, the Br concentrations in groundwaters fit well with those in the adjacent porewaters, except for the mismatch in the Muschelkalk aquifer of borehole BOZ1-1. Let us note that this groundwater sample was strongly contaminated by the drilling fluid (Wersin et al., 2022).

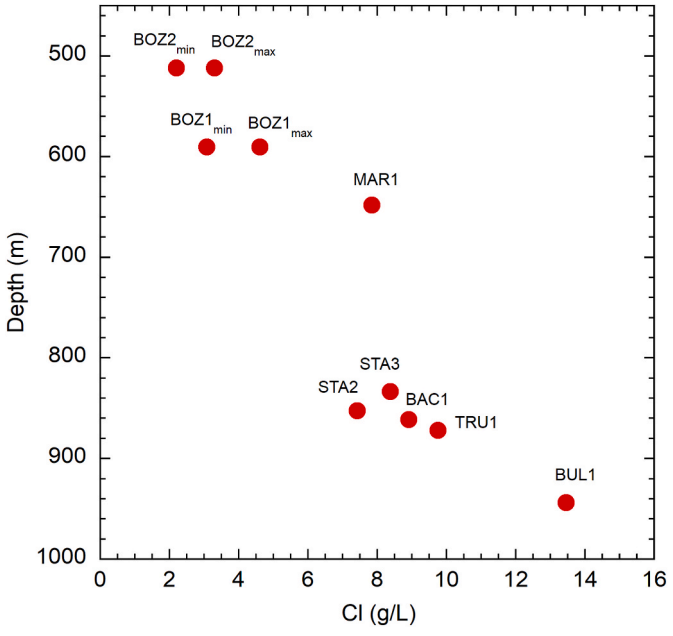

Fig. 4. Cl concentrations (g/L) in the centre of the Opalinus Clay as a function of depth shown for the different boreholes. Values based on aqueous extraction data.

4.3. Br/Cl ratios

Profiles of Br/Cl ratios (represented as 1000*Br/Cl in molar units) are depicted in Fig. 6. Overall, profiles are much smoother and uncertainty ranges are smaller compared to the single component profiles. This is because the ratios can be calculated directly from the aqueous extract data, and there is no need to account for water content and anion-accessible porosity with their large uncertainties. Thus, the smoothness of the Br/Cl profiles clearly indicates that much of the scatter seen in the Cl and Br profiles is due to the limited understanding of anion accessibility in the pore space of argillaceous-calcareous-silty rocks and due to the small water content and its heterogeneity on the cm scale in some parts of the profiles, in particular in large parts of the Triassic (mainly in limestones and evaporites) and in the Malm (limestones). It is also worth noting that all methods (AqEx, SQ, AD) yield more consistent results in comparison to the profiles of the individual anions.

JO study area: In the Malm-Dogger section, both boreholes show the same slightly decreasing depth trend but remain close to the seawater ratio in the upper part of the profile. In the Malm section, the profile is rather scattered, which is probably due to methodological reasons (low porosity and therefore a potential release of anions from fluid inclusions is more significant). BOZ1-1 shows an increase in Br/Cl ratios in the Lower Keuper, peaking in the evaporites at the footwall of this formation, followed by a sharp decrease towards the Muschelkalk aquifer. In the case of BOZ2-1, a more moderate positive excursion of the porewater profile is observed in the Upper Keuper in the zone of the aquifer, showing a mismatch with regard to the groundwater Br/Cl ratio (caused by a Br concentration in the groundwater that is well below that of porewaters at the same level, see Fig. 5).

NL study area: The four profiles shown in Fig. 6 show several commonalties but also evident differences. One commonalty is the presence of a central zone in all profiles with strictly constant (BUL1-1, STA3-1) or mildly decreasing (STA2-1, BAC1-1) Br/Cl ratios with depth. Such linear profiles can be taken as evidence of a long-term diffusive equilibration and are likely the oldest geochemical signature (at least in relative terms) because of the distance to the embedding aquifers. The linear sections extend from the centre of the Keuper (BAC1-1, STA3-1) or the base of the OPA (STA2-1) across the Opalinus Clay and the Dogger above the Opalinus Clay. In the case of BUL1-1, the trend is broken at the base of the reef limestones of the 'Herrenwis Unit'. In overlying Malm, the scatter of the data is slightly more strongly expressed, but this may be due to a possible contribution of anions from fluid inclusions in the limestones. In the lower Keuper and the Upper Muschelkalk, Br/Cl ratios tend to increase substantially, with a maximum in the evaporites close to the base of the Keuper, before values decrease again towards the Muschelkalk aquifer. The conspicuous exception is BUL1-1 where no such increase was found (see following section).

The main difference between the four boreholes are the absolute values of Br/Cl in the linear central parts of the profiles. These are slightly below the seawater ratio in the western boreholes BAC1-1 and STA2-1, at the seawater ratio of about 1.5×10^{-3} in STA3-1 but substantially lower (0.7×10^{-3}) in the easternmost borehole BUL1-1. It is remarkable that such contrasting signatures are found over a distance of only 2.8 km between STA3-1 and BUL1-1. It appears that the boundary conditions that led to the establishment of the linear segments remained different at the two sites over geological periods of time.

ZNO study area: Similar to the NL area, the central part of the profiles (Lias and Dogger) shows a conspicuously constant Br/Cl ratio, but the

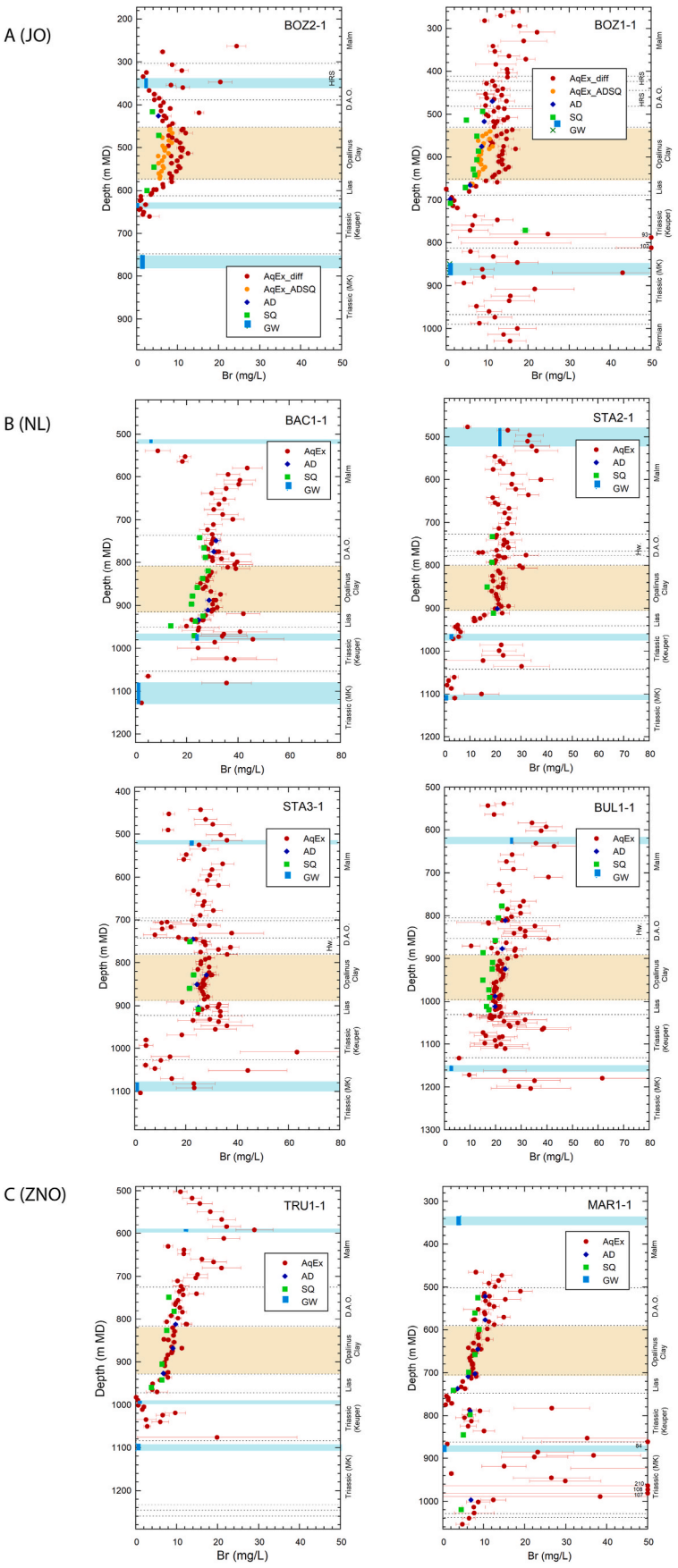

(caption on next page)

Fig. 5. Br profiles for study areas JO (A), NL (B) and ZNO (C). Opalinus Clay highlighted in beige. For JO boreholes, two variants for scaling of the AqEx (aqueous extraction) data are shown as detailed in the text. Blue bars for groundwater represent best estimates for position of major inflow zones. AD: advective displacement data, SQ: squeezing data, GW: groundwater data. MK: Muschelkalk, D.A.O.: Dogger above Opalinus Clay, HRS: Hauptrogenstein, Hw.: 'Herrenwis Unit'. Groundwater data are preliminary, minor changes for final data due to additional correction procedure for drlling fluid contamination are possible.

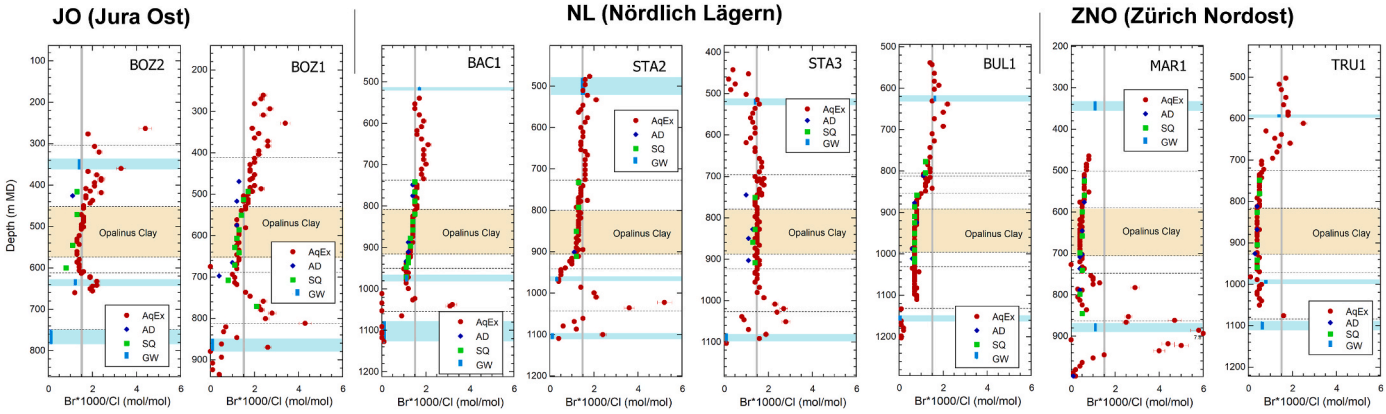

Fig. 6. Br/Cl profiles (molar ratios) for study areas JO (A), NL (B) and ZNO (C). Opalinus Clay highlighted in beige. Grey line: Br/Cl ratio of modern seawater. Blue bars for groundwater represent best estimates for position of major inflow zones. AqEx: aqueous extraction data, AD: advective displacement data, SQ: squeezing data, GW: groundwater data. Groundwater data are preliminary, minor changes for final data due to additional correction procedure for drlling fluid contamination are possible.

value of 0.4×10^{-3} in both boreholes is even lower than that of BUL1-1. Data for the Malm (available for TRU1-1 only) trend towards the seawater value of 1.5×10^{-3} and show a similar degree of scatter as in area NL. The Malm groundwater in MAR1-1 is more dilute compared to that in TRU-1, suggesting a larger meteoric influence, which is supported by stable water isotope data (Gimmi et al., 2023). Below the Keuper aquifer (groundwater only sampled in TRU1-1, but expected to be also present in MAR1-1; see Section 4.1), the Br/Cl ratio becomes more variable in comparison with the quite constant values at shallower levels. A distinct positive excursion of Br/Cl is seen in the Triassic of MAR1-1. The maximum value of 7.8×10^{-3} is located just below the groundwater sample, which has a much lower ratio of 1.1×10^{-3}. The reason for this inconsistency is not evident at this stage. The Br/Cl ratio decreases strongly with depth again in the lower Muschelkalk units to values well below modern seawater.

4.4. Regional interpretation of Br/Cl ratios

In addition to other data, such as stable water isotopes, the Br/Cl ratio can be used to discuss genetic aspects of the analysed porewaters and groundwaters (Kharaka and Hanor 2014). Tracer signals in the Mesozoic rock sequence depend among other factors on aquifer activation (and de-activation) times, marine transgression and regression periods in the Tertiary and impacts of uplift and erosion as well as glaciations in the Quaternary, all of which may affect paleo-flow and hydrochemistry. Moreover, dissolution phenomena in the evaporites of the Lower Muschelkalk related to non-uniformly distributed halite beds across the study areas clearly affected the Cl signals and explain the low Br/Cl ratios in the Muschelkalk aquifer.

The groundwater sampled in the nearest aquifer above the Opalinus Clay (Malm or Hauptrogenstein) typically has Br/Cl ratios indicating a marine component, which may be related to the last marine transgression during the sedimentation of the Upper Marine Molasse at 18–20 Ma (Waber and Traber 2022). The lower Br/Cl ratio observed in porewaters and groundwaters from borehole MAR1-1 is a prominent exception to this rule. In general, the data of porewaters and Malm groundwaters agree well, except for the JO study area, where the Br/Cl ratios of porewaters overlying the Opalinus Clay are somewhat above the marine value.

In the centre of the aquitard sequence, the porewater of the Lias and Dogger (sometimes extending into the upper Keuper) shows a trend from marine Br/Cl ratios (i.e. close to a value of 1.5×10^{-3} on a molar basis) in the western boreholes to lower values in the east (Fig. 6). There is no obvious correlation with the chloride concentration in the porewater, the occurrence of halite in the lower Muschelkalk or the hydrogeological conditions in the adjacent aquifers. The Br/Cl ratio in the Opalinus Clay likely reflects conditions that predate the current hydrogeochemical environment in the embedding aquifers, as also indicated from modelling (see section below). The scatter of the data in this section is conspicuously low, and the Br/Cl values are constant or show only limited trends with depth. Extended periods of time are needed to establish such conditions via diffusion.

In the majority of the boreholes, the maximum Br/Cl ratio well above the marine ratio is observed approximately at the base of Keuper (Fig. 6). The lower Keuper is mainly evaporitic and contains abundant anhydrite, and the high Br/Cl-ratios may originate from the evaporation of seawater beyond the onset of halite precipitation (Fontes and Matray 1993; Kharaka and Hanor 2014). While halite was not observed in the Keuper of the region, Hartmann (1925) described mirabilite and epsomite from an old mine shaft a few km to the southeast of the JO study area, which supports the presence of highly evaporated seawater and is consistent with the high Br/Cl ratios. The preservation of these ratios, together with the presence of highly soluble evaporitic minerals since the time of deposition, is remarkable but in line with the extremely low porosity (and therefore low diffusion coefficients) in the anhydrite-rich rocks (Mazurek et al., 2023). Moreover, the massive gradients of the $\delta^{18}O$ and $\delta^{2}H$ profiles observed across the evaporitic sections (Gimmi et al., 2023) are taken as an indication for a high sealing capacity. Note that the BUL1-1 borehole does not indicate this trend to high Br/Cl ratios in the Keuper, and this may be interpreted either by an absence of evolved evaporitic waters in this area or by the obliteration of this signal by prolonged diffusive exchange processes.

In the Muschelkalk aquifer, the chloride concentrations of the groundwater samples range from a few tens of mg/L up to 86 g/L (Fig. 3), and the Br/Cl ratios are well below the marine value. It is important to note that all Muschelkalk groundwater samples show a strong cold climate component with similar stable water isotope signals (Gimmi et al., 2023), regardless of their Cl concentrations. At least for

the chloride-rich groundwaters, but possibly for all, halite dissolution along the flow path is the likely source of salinity, given the presence of massive halite in the Zeglingen Formation, about 60–70 m below the Muschelkalk aquifer. This interpretation is supported by $\delta^{37}Cl$ data, which yielded similar values for groundwater and underlying halite at the three sites where analyses were performed (BOZ1-1, STA3-1, BUL1-1; see Wersin et al., 2022; Aschwanden et al., 2023; Mazurek et al., 2021).

4.5. Tracer modelling

Transport simulations for one example borehole from each study area (BOZ2-1, STA2-1 and TRU1-1) were performed according to the procedure outlined in section 3.5 and Appendix B1 (SM). The simulations for Cl and Br were built on the modelling study carried out for $\delta^{18}O$ and $\delta^{2}H$ (Gimmi et al., 2023) in which timings of changing aquifer signals could be inferred from simulations using the available paleo-hydrogeological and hydrochemical information.

In the first step, it was assumed that near-steady profiles were established before the activation of the various aquifers and the recent evolution of the porewaters. These initial compositions correspond to the highest present-day porewater Cl concentrations in the centre of the Opalinus Clay in each profile (Section 3.5). Upon attainment of steady-state conditions, groundwater signals of the upper aquifer (Malm/HRS) were switched to present day values (HRS in BOZ2-1: 0.35 Ma ago, Malm in STA2-1: 1.6 Ma ago, Malm in TRU1-1: first switch to lower values 4.65 Ma ago, second switch to present-day values 0.15 Ma ago, see Supplementary Material). The timing of the changing boundary conditions was set according to the modelling results for the stable water isotope signals. The switch to present-day values in the Keuper was set to 0.15 Ma before present for BOZ2-1, 0.1 Ma b.p. for STA2-1 and 0.65 Ma b.p. for TRU1-1. The change in the lower boundary (MK) to present day values was considered to occur very recently, in line with current knowledge on this aquifer (Waber and Traber, 2022), thus at 0.08 Ma b.p. for STA2-1 and 0.02 Ma b.p. for TRU1-1 (time not constrained for BOZ2-1 due to lack of data in lower part).

Overall, the simulations match both the Cl and Br profiles well, especially in the central parts and towards the Keuper aquifer (Fig. 7). This underlines the robustness of the underlying data on one hand and confirms the very similar diffusion rates of both anions on the other. Furthermore, the fact that the anion profiles can be adequately modelled with the same evolution times as applied for the stable water isotope tracers supports the adequacy of the modelling approach despite its simplified assumptions and boundary conditions. The general tendencies of the longer evolution times for the upper aquifers, but relatively recent (<1 Ma) evolution times in the lower aquifers are in line with the current understanding of the system, that is, longer times for the Malm boundary condition (except for an additional change for TRU1-1, and lower times for the HRS boundary in BOZ2-1), intermediate times for the Keuper boundary condition, and shortest times for Muschelkalk. The evolution times used here for the change of the signature in the Keuper aquifer of TRU1-1 are similar as those found for the BEN and SLA-1 boreholes in or near the ZNO area (ca. 0.55 Ma, with a range of ca. 0.5–1 Ma; Gimmi and Waber, 2004; Gimmi et al., 2007; Wersin et al., 2018).

The generally good match of Br/Cl ratios supports the simplified initial conditions that are thought to have resulted from the earlier evolution. Exceptions are the high Br/Cl ratios above the MK aquifer in STA2-1 and the tendency to higher values in the upper part of the profile for BOZ2-1. These likely reflect old signal trends which are not captured by the model. But, the partly large scatter of the data in these zones makes it generally difficult to match the model.

It should be noted that in the case of BOZ2-1 the considered concentrations and timing of changing groundwater signals only matched the variant in which anion-accessible porosities were based on AD/SQ data. With the variant based on porosities from diffusion experiments, the timing of the changing Hauptrogenstein aquifer signals (2.1 vs. 0.35 Ma) and the Keuper aquifer activation (0.3 vs. 0.15 Ma) needed to be adjusted to obtain a reasonable fit. Thus, it appears that for BOZ2-1 anion profiles based on AD/SQ data are superior as they lead to full consistency with times derived from stable water isotope tracers, while the profiles based on anion-accessible porosities from through-diffusion experiments would indicate somewhat longer evolution times compared to those of the water tracers. On the other hand, diffusion-based anion-accessible porosities for BOZ1-1 and BOZ2-1 from the JO study area appear closer to predicted ones based on double layer theory as discussed by Zwahlen et al. (2023). Thus, uncertainty with respect to anion-accessible porosity fractions remains regarding the two boreholes of JO which display the lowest salinities of all the studied deep boreholes. The differences observed here for the two different variants could also be related to uncertainties in the modelling, as for instance those related to the assumed initial conditions or the step-function used when changing aquifer signatures.

5. Conclusions

The deep drilling programme carried out in three study areas for the geological disposal of radioactive waste in the Opalinus Clay in northern Switzerland enabled to obtain highly resolved chloride and bromide profiles from the host rock, its low-permeable confining units as well as the overying Malm and underlying Triassic units. Systematic and comparable patterns are observed, suggesting common paleo-hydrogeological evolution paths for all three study areas. The scatter observed in the anion profiles is explained by the uncertainty in the estimation of the anion-accessible porosity fraction on one hand and in the porosity data in the case of low-porosity calcareous rocks on the other.

Differences between these study areas are, however, also evident. Thus, ZNO shows very similar Cl and Br profiles in all boreholes, at least for the Jurassic sequence, including also data from two older boreholes (Benken and Schlattingen-1). The Cl and Br profiles in the investigated Jurassic sequence can be explained by diffusive exchange between the porewaters and the groundwaters in the bounding Malm and Keuper aquifers, as shown by numerical modelling.

NL shows the most variable patterns between individual boreholes. Two of the boreholes (BUL1-1 and STA3-1) do not show any influence of a Keuper aquifer, as confirmed by the profiles of stable water isotopes and low transmissivities in that zone. For the other two boreholes (STA2-1, BAC1-1), an influence of the Keuper aquifer on anion profiles is indicated and supported by stable water isotopes, although in the case of BAC1-1 only a very weak effect is seen (possibly due to slow flow of water or comparably longer interaction time). Overall, the profiles in the OPA and confining units also corroborate the importance of diffusive exchange with the bounding aquifers in the overlying Malm and the underlying Keuper and/or Muschelkalk.

The westernmost shallow study area JO indicates the influence of the Keuper aquifer on the anion profiles for both boreholes. The overlying Hauptrogenstein aquifer also affected porewater tracers in the BOZ2-1 borehole while such effect is not observed for BOZ1-1, which is in line with the $\delta^{2}H$ and $\delta^{18}O$ profiles. Numerical modelling carried out on BOZ2-1 confirms that diffusive exchange having occurred between the Hauptrogenstein and Keuper aquifers can explain Cl and Br profiles.

The Br/Cl profiles show much smoother patterns in comparison to the profiles of the individual ions. This is due to the fact that they do not depend on assumptions pertinent to anion accessibility that are needed to calculate free-water concentrations from aqueous-extract data, and also because local sample heterogeneity is not relevant for ion ratios. Thus, Br/Cl profiles provide complementary information to that obtained from stable water isotopes, e.g. on the origin of salinity. Besides diffusive exchange between porewater and groundwater having occurred during the Quaternary period, older signals, originating from the evaporites in the Triassic, have left their local imprint to a variable

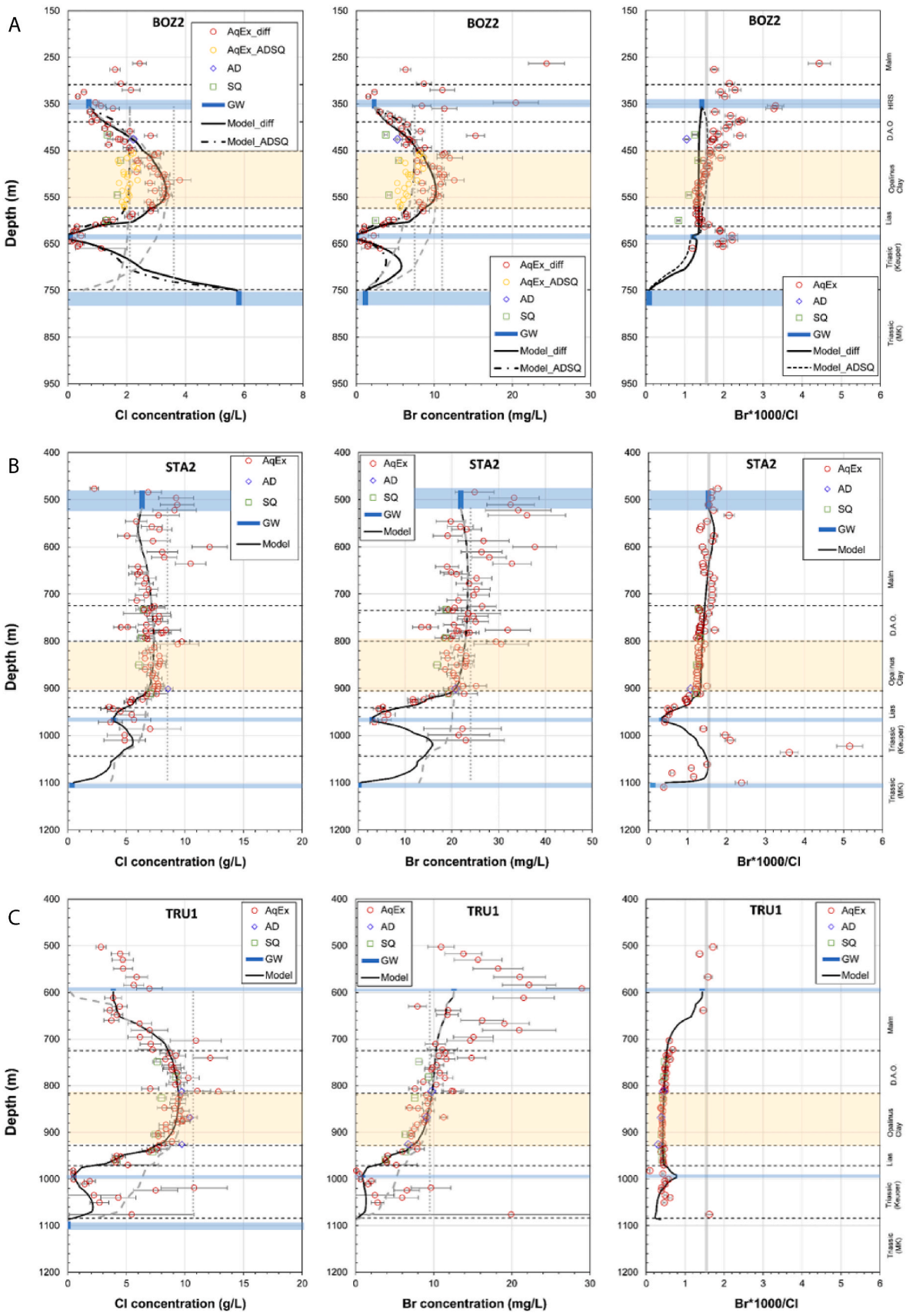

Fig. 7. Comparison of measured and simulated Cl, Br and Br/Cl in porewater and groundwater for (a) BOZ2-1 in JO, (b) STA2-1 in NL, and (c) TRU1-1 in ZNO. The dotted light grey line shows the used initial condition at the indicated time before present (b.p.), the dashed grey line the situation before the activation of the Keuper boundary condition, and the solid black line the final situation at present.

degree. Thus, halite dissolution in the lower Muschelkalk has induced low Br/Cl ratios in the porewaters in that formation and in the overlying aquifer. Conversely, the high Br/Cl ratios observed in the anhydrite-bearing lower Keuper in some of the boreholes are interpreted as an old signal originating from highly evolved evaporites. Moreover, a marine source, perhaps from the Tertiary marine transgression periods, seems to have variably affected the Jurassic sequence. A regional trend with Br/Cl ratios in the OPA and upper confining unit below that of seawater in the east, shifting to Br/Cl close to seawater towards the west can be inferred.

A systematic trend to higher Cl average concentrations in the OPA with increasing current average depth of the OPA is observed. This does not reflect recent infiltration conditions but is rather related to the preservation of an older paleo-hydrogeological signal.

The recent evolution (<1 Ma) of anionic tracers in the porewater could be adequately represented by a diffusion model with the same evolution times as derived from the stable water isotope tracers (Gimmi et al., 2023). This underlines the robustness of the modelling approach despite its simplicity.

Overall, the methodology adopted for the study of a potential host rock for radioactive waste disposal has enabled to obtain a unique dataset of anionic tracer profiles comprising an 800 m thick argillaceous sequence at regional scale. The findings provide a solid basis for the understanding of the regional paleo-hydrogeology. In particular, the Br/Cl ratios yield evidence of the impact of salt dissolution on the composition of the porewaters and groundwaters of the Muschelkalk. Finally, this study serves as benchmark for future investigations in clay-rich rocks foreseen as host rocks for nuclear waste repositories.

Declaration of competing interest

The authors declare that they have no known competing financial interests or personal relationships that could have appeared to influence the work reported in this paper.

Data availability

Data will be made available on request.

Acknowledgements

This study was part of the large deep drilling campaign 2019–2022 in northern Switzerland led by the Swiss National Cooperative for the Disposal of Radioactive Waste (Nagra). A number of international teams have contributed to the successful outcome of this campaign. For the present study, we would particularly like to thank A. Jenni, M. Kiczka, D. Rufer, U. Mäder, N. Waber, P. Bähler, C. Pichler, L. Camesi, U. Eggenberger, J. Gajic, M. Wolffers, A. Zappatini and F. Gfeller (University of Bern) for their contributions and fruitful discussions. We acknowledge Hydroisotop GmbH (Joy Ianotta, Florian Eichinger, Gesine Lorenz) for providing groundwater data. We further express our thanks to T. Oyama (CRIEPI, Japan) for support in porewater squeezing experiments and to Andreas Gautschi for reviewing an earlier version of this manuscript. Financial support by Nagra is acknowledged.

Appendix A. Supplementary data

Supplementary data to this article can be found online at https://doi.org/10.1016/j.apgeochem.2023.105845.

References

Altmann, S., Tournassat, C., Goutelard, F., Parneix, J.-C., Gimmi, T., Maes, N., 2012. Diffusion-driven transport in clayrock formations. Appl. Geochem. 27, 463–478.

Aschwanden, L., Camesi, L., Gaucher, E., Gimmi, T., Jenni, A., Kiczka, M., Mäder, U., Mazurek, M., Rufer, D., Waber, H.N., Wersin, P., Zwahlen, C., Traber, D., 2023. TBO Stadel-3-1: Data Report Dossier VIII. Rock Properties, Porewater Characterisation and Natural Tracer Profiles. Nagra Arbeitsbericht NAB 22-01, Nagra, Wettingen, Switzerland.

Bensenouci, F., Michelot, J.L., Matray, J.M., Savoye, S., Massault, M., Vinsot, A., 2014. Coupled study of water-stable isotopes and anions in porewater for characterizing aqueous transport through the Mesozoic sedimentary series in the eastern Paris Basin. Mar. Petrol. Geol. 53, 88–101.

Bock, H., Dehandschutter, B., Martin, C.D., Mazurek, M., De Haller, A., Skoczylas, F., Davy, C., 2010. Self-sealing of fractures in argillaceous formations in the context of geological disposal of radioactive waste. In: Review and Synthesis. Nuclear Energy Agency, OECD, Paris.

Fontes, J.C., Matray, J.M., 1993. Geochemistry and origin of formation brines from the Paris Basin. France. Chem. Geol. 109, 149–175.

Gimmi, T., Waber, H.N., 2004. Modelling of Tracer Profiles in Pore Water of Argillaceous Rock in the Benken Borehole: Stable Water Isotopes, Chloride and Chlorine Isotopes. Nagra Technical Report 04-05, Nagra, Wettingen, Switzerland.

Gimmi, T., Waber, H.N., Gautschi, A., Rübel, A., 2007. Stable water isotopes in pore water of Jurassic argillaceous rocks as tracers for solute transport over large spatial and temporal scales. Water Resour. Res. 43, W04410.

Gimmi, T., Aschwanden, L., Waber, H.N., Gaucher, E.C., Ma, J., Traber, D., 2023. Lateral and vertical variability of $\delta^{18}O$ and $\delta^{2}H$ in porewater of a Mesozoic rock sequence and implications for large-scale transport regimes. Appl. Geochem. 105846 https://doi.org/10.1016/j.apgeochem.2023.105846.

Gmünder, C., Malaguerra, F., Nusch, S., Traber, D., 2013. Regional Hydrogeological Model of Northern Switzerland, Nagra Arbeitsbericht 13-23, Nagra, Wettingen, Switzerland.

Hartmann, A., 1925. Die Mineral- und Heilquelle des Kantons Aargau. Mitt. Aarg. Naturf. Gesellsch., Heft 17.

Hendry, J.M., Barbour, S.L., Schmeling, E.E., Mundle, S.O.C., Huang, M., 2016. Fate and transport of dissolved methane and ethane in cretaceous shales of the Williston basin. Canada. Wat. Resourc. Res. 52, 6440–6450.

Horseman, S.T., Higgo, J.J.W., Alexander, J., Harrington, J.F., 1996. Water, Gas and Solute Movement through Argillaceous Media. NEA, OECD, Paris. Report CC-96/1.

Kharaka, Y., Hanor, J., 2014. 5.16 Deep fluids in the continents: I. Sedimentary Basins in Treatise on Geochemistry 471–515.

Kiczka, M., Wersin, P., Mazurek, M., Zwahlen, C., Jenni, A., Mäder, U., Traber, D., 2023. Porewater composition in clay rocks explored by advective displacement and squeezing experiments. Appl. Geochem. 105838. https://doi.org/10.1016/j.apgeochem.2023.105838.

Lorenz, G.D., Pechstein, A., Stopelli, E., 2022. Borehole BUL1-1 (Bülach-1-1): Fluid Sampling and Analytical Hydrochemical Data Report. Nagra Arbeitsbericht NAB 21-23. Nagra, Wettingen, Switzerland.

Mäder, U., 2018. Advective displacement method for the characterisation of pore water chemistry and transport properties in claystone. Geofluids 2018, 1–11.

Mazurek, M., Alt-Epping, P., Bath, A., Gimmi, T., Waber, H.N., 2009. Natural Tracer Profiles across Argillaceous Formations: the CLAYTRAC Project. Nuclear Energy Agency, OECD, Paris, p. 361.

Mazurek, M., Alt-Epping, P., Bath, A., Gimmi, T., Waber, N., Buschaert, S., De Cannière, P., De Craen, M., Gautschi, A., Savoye, S., Vinsot, A., Wemaere, Wouters, L., 2011. Natural tracer profiles across argillaceous formations. Appl. Geochem. 26, 1035–1064.

Mazurek, M., Gimmi, T., Zwahlen, C., Aschwanden, L., Gaucher, E.C., Kiczka, M., Rufer, D., Wersin, P., Marques Fernandes, M., Glaus, M., Van Loon, L.C., Traber, D., Schnellmann, M., Vietor, T., 2023. Swiss deep drilling campaign 2019–2022: Geological overview and rock properties with focus on porosity and pore-space architecture. Appl. Geochem. 105839 https://doi.org/10.1016/j.apgeochem.2023.105839.

Mazurek, M., Oyama, T., Wersin, P., Alt-Epping, P., 2015. Pore-water squeezing from indurated shales. Chem. Geol. 400, 106–121.

Mazurek, M., Aschwanden, L., Camesi, L., Gimmi, T., Jenni, A., Kiczka, M., Rufer, D., Waber, H.N., Wanner, P., Wersin, P., Traber, D., 2021. TBO Bülach-1-1: Data Report Dossier VIII. Rock Properties, Porewater Characterisation and Natural Tracer Profiles. Nagra Arbeitsbericht NAB 20-08, Nagra, Wettingen, Switzerland.

Nagra, 2001. Sondierbohrung Benken Untersuchungsbericht. Nagra Technischer Bericht NTB 00-01. Nagra, Wettingen, Switzerland.

Nagra, 2014. SGT Etappe 2: Vorschlag weiter zu untersuchender geologischer Standortgebiete mit zugehörigen Standortarealen für die Oberflächenanlage. Geologische Grundlagen. Dossier VI: Hydrogeologische Verhältnisse. Nagra Technical Report NTB 14-02. Nagra, Wettingen, Switzerland.

Patriarche, D., Michelot, J.-L., Ledoux, E., Savoye, S., 2004a. Diffusion as the main process for mass transport in very low water content argillites: 1. Chloride as a natural tracer for mass transport—diffusion coefficient and concentration measurements in interstitial water. Water Resour. Res. 40, W01516.

Patriarche, D., Ledoux, E., Michelot, J.-L., Simon-Coinçon, R., Savoye, S., 2004b. Diffusion as the main process for mass transport in very low water content argillites: 2. Fluid flow and mass transport modeling. Water Resour. Res. 40, W01517.

Pearson, F.J., 1999. What is the porosity of a mudrock?. In: Aplin, A.C., Fleet, A.J., Macquaker, J.H.S. (Eds.), Muds and Mudstones: Physical and Fluid Flow Properties, vol. 158. Geological Society, London, Special Publications, pp. 9–21.

Pearson, F.J., Arcos, D., Bath, A., Boisson, J.Y., Fernández, A.M., Gäbler, H.-E., Gaucher, E., Gautschi, A., Griffault, L., Hernán, P., Waber, H.N., 2003. Geochemistry of Water in the Opalinus Clay Formation at the Mont Terri Rock Laboratory. Federal Office for Water and Geology, Bern. Series No. 5.

Rufer, D., Stockhecke, M., 2021. In: Field Manual: Drill Core Sampling for Analytical Purposes. Nagra Arbeitsbericht NAB 19-13 Rev. 1, Nagra, Wettingen, Switzerland.

Rufer, D., Waber, H.N., Traber, D., 2023. Vertical and lateral distribution of helium in porewater in the Swiss Molasse Basin – a comparative investigation across multiple

boreholes. Appl. Geochem. 105836 https://doi.org/10.1016/j.apgeochem.2023.105836.
RWI, 2020. SGT-E3 Deep Drilling Campaign (TBO): Experiment Procedures and Analytical Methods at RWI, University of Bern (Rock-Water Interaction group, University of Bern, Switzerland Version 1.0, April 2020). Nagra Arbeitsbericht NAB 20-13, Nagra, Wettingen, Switzerland.
Schwarz, R., Schlickenrieder, L., Müller, H.R., Köhler, S., Pechstein, A., Vogt, T., 2021a. TBO Trüllikon-1-1: Data Report, Dossier VII: Hydraulic Packer Testing. Nagra Arbeitsbericht NAB 20-09, Nagra, Wettingen, Switzerland.
Schwarz, R., Hardie, S.M.L., Müller, H.R., Köhler, S., Pechstein, A., 2021b. TBO Marthalen-1-1: Data Report, Dossier VII: Hydraulic Packer Testing. Nagra Arbeitsbericht NAB 21-20, Nagra, Wettingen, Switzerland.
Schwarz, R., Schlickenrieder, L., Vogt, T., 2021c. TBO Bülach-1-1: Data Report, Dossier VII: Hydraulic Packer Testing. Nagra Arbeitsbericht NAB 20-08, Nagra, Wettingen, Switzerland.
Schwarz, R., Willmann, M., Fisch, H., Schlickenrieder, L., Voss, M., Pechstein, A., 2022a. TBO Stadel 3-1: Data Report, Dossier VII: Hydraulic Packer Testing. Nagra Arbeitsbericht NAB 22-01, Nagra, Wettingen, Switzerland.
Schwarz, R., Beauheim, R., Hardie, S.M.L., Pechstein, A., 2022b. TBO Stadel 2-1: Data Report, Dossier VII: Hydraulic Packer Testing. Nagra Arbeitsbericht NAB 22-02, Nagra, Wettingen, Switzerland.
Schwarz, R., Beauheim, R., Hardie, S.M.L., Voss, M., Pechstein, A., 2022c. TBO Bözberg-1-1: Data Report, Dossier VII: Hydraulic Packer Testing. Nagra Arbeitsbericht NAB 21-21, Nagra, Wettingen, Switzerland.
Schwarz, R., Willmann, M., Reinhardt, S., Hardie, S.M.L., Voss, M., Pechstein, A., 2022d. TBO Bözberg-2-1: Data Report, Dossier VII: Hydraulic Packer Testing. Nagra Arbeitsbericht NAB 21-22, Nagra, Wettingen, Switzerland.
Traber, D., 2013. Untere Rahmengesteine des Opalinustons: hydrogeologische Einheiten, Gesteinsparameter und Mächtigkeiten. Nagra Arbeitsbericht NAB 12-40. Nagra, Wettingen, Switzerland.
Van Loon, L.R., Bunic, M.A., Frick, P, Glaus, S., Wüst, R.A.J., 2023. Diffusion coefficients for HTO, ^{36}Cl and ^{22}Na in the heterogeneous Mesozoic rocks of Northern Switzerland: measurement of effective diffusion coefficients and capacity factors. Appl. Geochem. 105843 https://doi.org/10.1016/j.apgeochem.2023.10584.
Waber, H.N., Traber, D., 2022. Die Tiefengrundwässer in der Nordschweiz und im angrenzenden Süddeutschland: Beschaffenheit, Herkunft und unterirdische Verweilzeit. Nagra Technischer Bericht NTB 19-02. Nagra, Wettingen, Switzerland.
Waber, H.N., Heidinger, M., Lorenz, G., Traber, D., 2014. Hydrochemie und Isotopenhydrogeologie von Tiefengrundwässern in der Nordschweiz und im angrenzenden Süddeutschland. Nagra Arbeitsbericht NAB 13-63. Nagra, Wettingen, Switzerland.
Waber, H.N., Traber, D., Stopelli, E., 2023. TBO Trüllikon-1-1 (TRU1-1): Groundwater Hydrogeochemistry. Nagra Arbeitsbericht 23-24. Nagra, Wettingen, Switzerland.
Wersin, P., Mazurek, M., Mäder, U.K., Gimmi, T., Rufer, D., Lerouge, C., Traber, D., 2016. Constraining porewater chemistry in a 250 m thick argillaceous rock sequence. Chem. Geol. 434, 43–61.
Wersin, P., Gimmi, T., Mazurek, M., Alt-Epping, P., Pekala, M., Traber, D., 2018. Multicomponent diffusion in a 280 m thick argillaceous rock sequence. Appl. Geochem. 95, 110–123.
Wersin, P., Aschwanden, L., Camesi, L., Gaucher, E.C., Gimmi, T., Jenni, A., Kiczka, M., Mäder, U., Mazurek, M., Rufer, D., Waber, H.N., Zwahlen, C., Traber, D., 2022. TBO Bözberg 1-1: Data Report Dossier VIII. Rock Properties, Porewater Characterisation and Natural Tracer Profiles. Nagra Arbeitsbericht NAB 21-21. Nagra, Wettingen, Switzerland.
Zwahlen, C., Gimmi, T., Jenni, A., Kiczka, M., Mazurek, M., Van Loon, L., Mäder, U., Traber, D., 2023. Chloride accessible porosity fractions across the Jurassic sedimentary rocks of northern Switzerland. Appl. Geochem. 105841 https://doi.org/10.1016/j.apgeochem.2023.10584.